1-2021

Larval anatomy of monotypic painted ant nest frogs Lithodytes lineatus reveals putative homoplasies with the Leptodactylus pentadactylus group (Anura: Leptodactylidae)

Filipe A.C do Nascimento

Rafael O. de Sá
University of Richmond, rdesa@richmond.edu

Paulo C. de A. Garcia

Recommended Citation

do Nascimento, F. A. C., de Sá, R.O., and Garcia, P. C. de A. 2021. Larval anatomy of the monotypic genus Lithodytes reveals putative homoplasies with species of the Leptodactylus pentadactylus species group Anura: Leptodactylidae). Zoologischer Anzeiger 290 (1): 135–147, (https: //doi.org/10.1016/j.jcz.2020.12.003).

Zoologischer Anzeiger 290 (2021) 135–147

Contents lists available at ScienceDirect

Zoologischer Anzeiger

journal homepage: www.elsevier.com/locate/jcz

Research paper

Larval anatomy of monotypic painted ant nest frogs *Lithodytes lineatus* reveals putative homoplasies with the *Leptodactylus pentadactylus* group (Anura: Leptodactylidae)

Filipe A.C. do Nascimento [a, b, *], Rafael O. de Sá [c], Paulo C. de A. Garcia [b, d]

[a] Setor de Herpetologia, Museu de História Natural, Universidade Federal de Alagoas, Maceió, AL, Brazil
[b] Pós-Graduação em Zoologia, Instituto de Ciências Biológicas, Universidade Federal de Minas Gerais, Belo Horizonte, MG, Brazil
[c] Department of Biology, University of Richmond, Richmond, VA, USA
[d] Departamento de Zoologia, Instituto de Ciências Biológicas, Universidade Federal de Minas Gerais, Belo Horizonte, MG, Brazil

ARTICLE INFO

Article history:
Received 25 July 2020
Received in revised form
10 December 2020
Accepted 18 December 2020
Available online 23 December 2020

Keywords:
Tadpole
Chondrocranium
Internal oral anatomy
Leptodactylinae
Systematics
Evolution

ABSTRACT

The morphological diversity of anuran larvae made them an important source of information for evolutionary and systematic studies. For the monotypic frog genus *Lithodytes*, which has an interesting taxonomic history, including its past synonymizing with *Adenomera* and its placement as a subgenus of *Leptodactylus*, the information provided from its larvae can help to understand its systematics interrelationships and also provide insights about its evolutionary trajectories. Herein, we provide a detailed description of the larval morphology of *Lithodytes lineatus*, including novel data of internal morphology (buccopharyngeal cavity and skeleton), and discuss some morphological and evolutionary aspects in relation to other members of the subfamily Leptodactylinae. Despite the overall similar larval morphology with others members of the subfamily, we identified four autapomorphic traits for *Lithodytes* and seven purported homoplastic traits with a subclade of the *Leptodactylus pentadactylus* species group that likely evolved convergently. Some of these traits have been previously associated with a carnivorous diet. Putative homoplastic and autapomorphic characters served as additional diagnostic traits for *Lithodytes*, supporting its recognition as a distinct genus within Leptodactylidae.

1. Introduction

The morphological diversity of anuran larvae and their deep divergence in relation to their adult morphology made them an important source of information for evolutionary and systematic studies (Bell & Wassersug, 2003; Haas, 2003; Púgener et al., 2003; Grosso et al., 2020). Along with the traditional use of external morphology characters, the increasingly wide use of those coming from internal traits have been shown to be quite informative (e.g., buccopharyngeal cavity, chondrocranial, and muscular anatomy). These can help to understand the morphological, functional, and ecological diversity of tadpoles (Svensson & Haas, 2005; Vera Candioti, 2007) but also to decipher their evolutionary trajectories in anuran systematics (Larson & de Sá, 1998; Miranda et al., 2014; Dias et al., 2019). Recent evidence corroborated the theory of adaptive decoupling between adult and larvae stages of frogs (Sherratt et al., 2017; Valero et al., 2017); consequently, understanding the diversity of tadpole morphology is critical for evolutionary studies.

The frog family Leptodactylidae currently consists of 223 species (Frost, 2020) allocated to three subfamilies (Leptodactylinae, Leiuperinae, and Paratelmatobiinae) with a combined distribution on the New World from southern United States to Argentina and Chile (de Sá et al., 2014). The family has a striking diversity of reproductive modes. Most species are foam-nesting builders and their tadpoles occupy different habitats, from general lentic forms (e.g., *Physalaemus* Fitzinger, 1826; Ceron & Santana, 2017; and *Pseudopaludicola* Miranda-Ribeiro, 1926; Andrade et al., 2018) to streams associated with rock outcrops habitats (some *Leptodactylus* Fitzinger, 1826; Heyer, 1995).

The monotypic leptodactylid genus *Lithodytes* Fitzinger, 1843 has an interesting taxonomic history. The genus *Adenomera* Steindachner, 1867 was placed in the synonymy of *Lithodytes* and

* Corresponding author. Setor de Herpetologia, Museu de História Natural, Universidade Federal de Alagoas, Maceió, AL, Brazil.
E-mail addresses: filipe.nascimento@mhn.ufal.br (F.A.C. Nascimento), rdesa@richmond.edu (R.O. de Sá), pcagarcia@gmail.com (P.C.A. Garcia).

https://doi.org/10.1016/j.jcz.2020.12.003
0044-5231/

Lithodytes as a subgenus of *Leptodactylus* (Heyer, 1998; Kokubum & Giaretta, 2005; Frost et al., 2006); however, they were treated as separate taxa in a large-scale Amphibia phylogeny of Pyron & Wiens (2011). Recently, a phylogenetic analysis with molecular and non-molecular characters, and a larger ingroup sampling, supported the monophyly of these three genera (de Sá et al., 2014). That study recognized *Lithodytes* as a valid genus based on (i) the absence of endotrophic larvae (present in *Adenomera*), (ii) the differences in adult morphology, and (iii) the high mitochondrial divergence among *Lithodytes lineatus* samples from Brazil and Peru (Fouquet et al., 2007). Currently, *Lithodytes* is considered as the sister group of *Adenomera* and this clade is sister to the clade consisting of *Hydrolaetare* Gallardo, 1963 and *Leptodactylus* (Pyron & Wiens, 2011; Fouquet et al., 2013; 2014; de Sá et al., 2014), forming the subfamily Leptodactylinae.

Lithodytes has a wide distribution throughout the Amazon basin, including transitional areas of Cerrado-Amazon and forest areas of the Brazilian Cerrado (see Thaler et al., 2020 for a compilation of known records). The genus consists of a single leaf-litter species, *L. lineatus* (Schneider, 1799), that lives in association with leaf-cutting ant nests of the species *Atta cephalotes* (Linnaeus, 1758) (Schlüter, 1980; Lamar & Wild, 1995). The ant nests are used as breeding sites and tadpoles complete their development in ponds associated with burrows of these nests (Schlüter et al., 2009). The coloration and diurnal habit of juveniles suggest the species to be mimetic with some toxic Dendrobatoidea, i.e., *Allobates femoralis* (Boulenger, 1884) and *Ameerega hahneli* (Boulenger, 1884) (Lamar & Wild, 1995; Duellman, 2005).

Regös & Schlüter (1984) compared aspects of normal and abnormal larval development of *L. lineatus*. Subsequently, its external tadpole morphology was briefly described (Lamar & Wild, 1995; Schlüter & Regös, 1996). Herein, we provide a detailed description of the larval morphology of *L. lineatus*, including novel data of internal morphology (buccopharyngeal cavity and skeleton), and discuss some morphological and evolutionary aspects in relation to other members of the subfamily Leptodactylinae.

2. Materials and methods

2.1. Specimens

We examined four tadpoles of *L. lineatus* deposited at the Museo de Zoología de la Pontificia Universidad Católica del Ecuador (QCAZ). Specimens are from Ecuador, collected at Orellana province (QCAZ 8334; 00°51′S, 76°16′W, WGS84; on January 1995), Napo province (QCAZ 9530; 01°02′S, 77°36′W, WGS84; on May 1994), and Pastaza province (QCAZ 25190, 29257, 01°24′S 77°59′W, WGS84, on April 2001). The identification of these tadpoles was based on their collection site, i.e., in leaf-cutting ant nests where the species breeds, along with their peculiar larval morphology (Lamar & Wild, 1995; Schlüter & Regös, 1996). We also examined tadpoles of the following Leptodactylinae frogs: *Adenomera* sp., *Adenomera thomei* (Almeida & Angulo, 2006), *Leptodactylus* cf. *latrans* (Steffen, 1815), *L. fuscus* (Schneider, 1799), *L. rhomomystax* Boulenger, 1884, *L. troglodytes* Lutz, 1926, *Leptodactylus pentadactylus* (Laurenti, 1768), *L. pustulatus* (Peters, 1870), *Leptodactylus labyrinthicus* (Spix, 1824), and *Leptodactylus vastus* Lutz, 1930 (supplementary materials SM.01). Identification of these species was made following one of the following procedures: (i) use of larvae from the same lot used in the original description of the tadpole, (ii) geographical distribution, and/or (iii) direct comparison with the original description.

2.2. External morphology

Measurements and analysis of external morphology were taken from all four tadpoles (stages 33, 39, and 40; Gosner, 1960); tadpole description is based on a stage 33 larva. The following measurements were taken: body length (BL), maximum tail height (MTH), tail length (TaL), tail muscle height (TMH), tail muscle width (TMW), and total length (TL) (*sensu* Altig & McDiarmid, 1999); body width at eye level (BWE), body width at nostril level (BWN), width of the dorsal gap of the oral disc (DGO), extranarial distance (EnD), extraorbital distance (EoD), eye diameter (ED), eye-nostril distance (END), intranarial distance (InD), intraorbital distance (IoD), maximum body height (MBH), maximum body width (MBW), narial diameter (ND), oral disc width (ODW), snout-nostril distance (SND), snout-spiracle distance (SSD), and spiracle-posterior body distance (SPD) (*sensu* Lavilla & Scrocchi, 1986); dorsal fin height (DFH) and ventral fin height (VFH) (*sensu* Grosjean, 2005); and spiracle length (SL), and vent tube length (VTL) (*sensu* Rodrigues et al., 2017). Additionally, we measured the angle of insertion of the dorsal fin (DFIA, *sensu* Pinheiro et al., 2012) and the angular orientation of the oral disc (ODAO). The later was adapted from Altig & Johnston (1989), as follow: oral disc position as almost ventral/ventral ($0° < x \leq 20°$), anteroventral ($21° < x \leq 40°$), and almost terminal/terminal ($x > 40°$). All measurements were taken using an ocular micrometer installed on a Leica® MZ6 stereomicroscope; except for TL which was measured with digital calipers (0.1 mm accuracy) and DFIA and ODAO that were measured with the aid of the ImageJ v. 1.50i software from photos taken using a digital camera installed on a Coleman® NSZ 405 stereomicroscope. Illustrations were made from multifocal photographs taken with a Leica M205 stereomicroscope. A few tadpole structures, e.g., oral disc, vent tube, and spiracle, were stained with methylene blue solution to enhance observation. Terminology of external morphology follows Altig & McDiarmid (1999). For coloration description, we use the terminology and corresponding color codes from Köhler (2012).

2.3. Buccopharyngeal cavity

Description of buccopharyngeal cavity was based on two tadpoles in stage 40. Specimens were dissected following Wassersug (1976) and prepared for scanning electron microscope (SEM) following standard procedures (Nascimento et al., 2020); terminology follows (Wassersug, 1976, 1980) . Examinations and photos were taken under a Quanta FEG 3D SEM at 5 kV.

2.4. Skeleton

Chondrocranial and hyobranchial apparatus descriptions were based on a tadpole in stage 39. The specimen was cleared and double-stained for bone and cartilage following standard protocol (Dingerkus & Uhler, 1977). The following measurements were taken: chondrocranium total length (CTL), chondrocranium maximum width (CMW), chondrocranium maximum height (CMH), *cornua trabeculae* length (CTrL), otic capsule length (OCL), otic capsule width (OCW), otic capsule height (OCH), *planum trabecularum* length (PTrL), and *planum trabecularum* width (PTrW) (*sensu* Alcalde & Rosset, 2003); *cornua trabeculae* maximum width (CTMW), *pars articularis quadrati* length (PAQL), *pars articularis quadrati* width (PAQW), *cartilago meckeli* length (CML), *cartilago meckeli* width (CMW), *cartilago infrarostralis* length (CIL), *cartilago infrarostralis* width (CIW), angle of *cartilago meckeli* relative to the main body axis (CMA), and angle of *cartilago infrarostralis* relative to the main body axis (CIA) (*sensu* Alcalde et al., 2011); and *processus anterior hyalis* length (PAHL) and *processus anterolateralis hyalis* length (PAlHL) (*sensu* Hass, 2003). All measurements were taken

using an ocular micrometer installed on a Leica® MZ6 stereomicroscope, except for MCA, IA, APCL, and AlPCL that were measured with the aid of the ImageJ v.1.50i software from photos taken using a digital camera installed on a Coleman® NSZ 405 stereomicroscope. Illustrations were made using a Leica MZ6 stereomicroscope with a camera-lucida attachment and editing in Adobe Photoshop® software. Terminology follows Larson & de Sá (1998) and Cannatella et al. (1999).

Character optimization was done using the parsimony algorithm in Mesquite 3.20 (Maddison & Maddison, 2016). The coding of characters was made from our examination of characters and from literature (see discussion).

3. Results

3.1. External morphology (stage 33)

Total length 34.6 mm (Fig. 1A–C). Body elliptical to rectangular in dorsal and ventral views (MBW/BL = 0.57), trapezoidal in lateral view, slightly wider than high (MBH/MBW = 0.80), with flat ventral body contour. Body length 40% of total length; maximum body width at the mid-third of the body and maximum body height on the posterior third. Snout rounded in dorsal and lateral views. Eyes located dorsally and directed dorsolaterally, eye diameter about 32% of interorbital distance, and 8% of maximum body width. Nostrils dorsal and directed dorsolaterally, with external opening circular surrounded by a discontinuous and cream/light colored marginal rim; nostril diameter about 20% of internarial distance and 5% of maximum body width; located almost midway between the snout tip and the eyes (END/SND = 1.18). Oral disc about 41% of the maximum body width, almost terminal (ODAO = 49.6°), with a midventral pleat (Fig. 1E and 4G). The labium bears a single row of marginal papillae (about 6 papillae/mm) with a gap on the upper labium (DGO/ODW = 0.69; about 18 papillae width), lacking submarginal papillae. Marginal papillae large; overall conical, elongated, and with rounded tip. Labial tooth row formula (LTRF) 2(2)/3(1); relative length of each row: A1 = A2 = P1=P2>P3. Length of P3 row about 65% of the other rows; rows A2 and P1 with medial

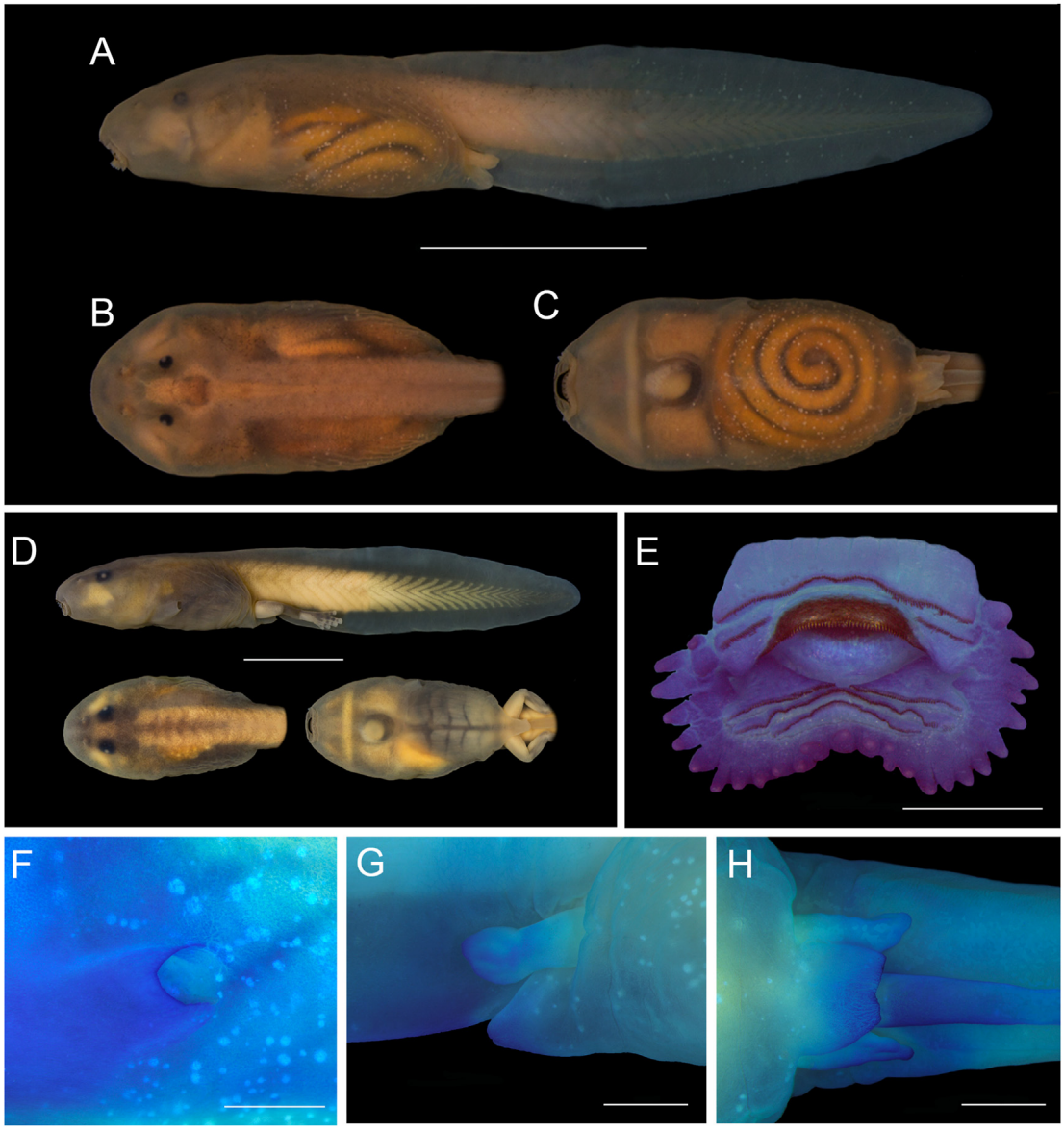

Fig. 1. Tadpole of *Lithodytes lineatus* at stage 33 (QCAZ 8334). (A) Lateral, (B) dorsal, and (C) ventral views (scale bar = 10 mm). (D) Tadpole at stage 39 (QCAZ 29257). (E) Oral apparatus, (F) spiracle in lateral view, (G) vent tube in lateral and (H) in ventral views (same specimen as in A, scale bar = 1 mm).

gaps (about 55% of the A2 length and about 6% of the P1 length, respectively). Jaw sheaths dark; upper jaw sheath arc-shaped and finely serrated (about 50 serrations/mm), serrations straight medially; lower jaw sheath V open-shaped with finely serrated edge (about 50 serrations/mm), serrations dorsally oriented. Spiracle sinistral, ventrolateral, opening on the middle third of the body (SPD/SSD = 0.61), directed posterodorsally and forming an angle of approximately 15° with the longitudinal body axis; inner wall absent and margin of the spiracle opening smooth (Fig. 1F). Vent tube with medial opening, overall tube of equal length and width, attached to the ventral fin and with a free distal tip; ventral and dorsal walls of equal length and margin of aperture smooth (Fig. 1G and H). Tail length about 60% of total length, maximum height greater than body height (MBH/MTH = 0.86), highest on the middle third. Tail tip rounded. Maximum tail musculature less than half the maximum tail height (TMH/MTH = 0.42), becoming progressively thinner posteriorly, i.e., beyond the anterior third, and extending to the tail tip; myosepta visible. Dorsal fin height one third of tail height (DFH/MTH = 0.29) and almost equal to ventral fin height (VFH/DFH = 1.05). Dorsal fin beginning at the body-tail junction, with a convex contour (DFIA = 8.9°); maximum height at the middle third of the tail. Origin of ventral fin concealed by the vent tube and convex contour that follows the longitudinal axis of the tail musculature; maximum height at middle third of the tail. A summary of larval measurements is provided in Table 1.

Coloration. In preservative, body and tail drab-gray (256). Superficial integument lacks melanophores, ventral body translucent. Innermost layers of the dorsum with scarce filiform melanophores in a reticulated pattern; melanophores also found ventrally over the peribranchial region and on epaxial region of the tail musculature. Fins translucent and lacking melanophores.

Variations. Ontogenetically, specimens at later stages (n = 3; stages 39 and 40; Fig. 1D) have a larger eye diameter than younger specimens (e.g., in stage 33 the relation ED/BWE was 0.09 while in stage 39–40 was = 0.17 ± 0.03). The coloration pattern also varies in older specimens. Body and lateral surfaces are Cinnamon (21) with the superficial integument and innermost layer of dorsum and lateral body walls having a high density of filiform melanophores in a mesh pattern. Ventral body and tail are Drab (19).

3.2. Buccopharyngeal cavity (stage 40)

*Buccal roof (*Fig. 2A and B*).* Buccal roof diamond-shaped, wider than long (buccal roof length/width about 1.4). Prenarial arena wide (length/width about 0.65), with two slightly curve-shaped ridges transversally located midway the jaw sheath and the choanae. Overall, the choanae are drop-shaped, located about 25% distance from jaw sheath to esophagus; maximum choanae length about 15% of buccal roof width; internarial distance about 3% of buccal roof width. Choanae oriented parallel from transverse plane; anterior wall thick, directed anteromedially (what gives the "drop" shaped of the choanae), with three conical prenarial papillae distributed along its lateral half, with the most lateral one three times longer than others, 2–3 additional pustules distributed on its medial half; posterior wall wider than high, with narial valve; narial valve projection present but not clearly distinct. Presence of concavities in the region bounded by the choana, lining by ciliated or microvillied tissue. Length of the postnarial arena similar to that of the prenarial arena; one pair of elongated postnarial papillae (width/length about 0.4) located closer to the choanae than the median ridge; aligned transversally, projecting anteromedially, and extending beyond the posterior wall of the choanae. Median ridge located about 45% of the distance from the jaw sheath to the esophagus; overall broad and pocket-like (width/length about 2.4), with a rectilinear margin and two distinct and short conical papillae medially on the margin; 5–6 pustules scattered on its ventral surface. One pair of elongated and triangular lateral ridge papillae with 3–5 secondary projections on its anterior margin, located anterolaterally to the median ridge and projecting over the postnarial papillae. Buccal roof arena (BRA) elliptical, delimited anteriorly by the median ridge and laterally and posterolaterally by 10–12 conical BRA papillae; about 30 pustules distributed on the BRA, in higher density posteriorly; two shorter lateral roof papillae. Glandular zone distinct, arc-shaped, medial portion length equivalent to 10% the buccal roof length; secretory pits distinct, scarcer laterally. Dorsal velum length equivalent to 15% the buccal roof length, interrupted medially, with small and barely visible pustulations on its posterior margin.

*Buccal floor (*Fig. 2C and D*).* Buccal floor triangular-shaped, slightly wider than long (buccal floor length/width about 0.9). Three pair of infralabial papillae; first pair of small, rostral papillae, following by a second pair of slightly longer, juxtaposed papillae, posteromedial on the midline, both conical and bearing 4–5 pustules distally, and a third pair posterolateral, on the *cartilago meckeli*, compressed and palp-shaped (Fig. 3). Lingual anlage bears four finger-like lingual papillae aligned transversally, lateral ones shorter and blunt, 4–5 pustules terminally along its body; additionally, a small fifth lingual papilla found anterior to the others in one of the specimens. Buccal floor arena (BFA) diamond-shaped, with about 25 conical papillae mostly distributed in two rows, one runs medially from the anterior edge of the BFA, following convergingly until the BFA posterior region; most papillae of the

Table 1
Measurements for external morphology of Lithodytes lineatus tadpoles (QCAZ 8334, 9530, 25190, 29257). Abbreviations: body length (BL), body width at eye level (BWE), body width at nostril level (BWN), dorsal fin height (DFH), dorsal fin insertion angle (DFIA), extranarial distance (EnD), extraorbital distance (EoD), eye diameter (ED), eye-nostril distance (END), intranarial distance (InD), intraorbital distance (IoD), maximum body height (MBH), maximum body width (MBW), maximum tail height (MTH), narial diameter (ND), oral disc angular orientation (ODAO), oral disc width (ODW), snout-nostril distance (SND), snout-spiracle distance (SSD), spiracle length (SL), spiracle-posterior body distance (SPD), tail length (TaL), tail muscle height (TMH), tail muscle width (TMW), total length (TL), vent tube length (VTL), ventral fin height (VFH), and width of the dorsal gap of the oral disc (DGO).

Measurements	Stage 33 (n = 1)	Stage 39 (n = 1)	Stage 40 (n = 2)
BL	13.7	17.5	17.0 ± 1.8 (15.8–18.3)
BWE	7.6	9.3	9.1 ± 0.8 (8.6–9.7)
BWN	5.2	6.4	6.2 ± 0.5 (5.8–6.6)
DFH	2.1	3.0	2.5 ± 0.5 (2.2–2.9)
DFIA	8.9	8.8	5.7 ± 1.0 (4.9–6.4)
DGO	2.2	3.1	2.8 ± 0.4 (2.5–3.1)
ED	0.7	1.8	1.5 ± 0.2 (1.3–1.6)
EnD	2.2	2.9	2.8 ± 0.2 (2.6–3.0)
END	1.4	1.6	1.6 ± 0.1 (1.5–1.6)
EoD	3.2	5.2	5.1 ± 0.5 (4.7–5.5)
InD	1.8	2.5	2.4 ± 0.4 (2.1–2.6)
IoD	2.1	2.2	2.2 ± 0.2 (2.1–2.4)
MBH	6.3	8.0	8.1 ± 1.0 (7.4–8.8)
MBW	7.8	11.2	16.2 ± 8.2 (10.3–22.0)
MTH	7.3	9.1	8.8 ± 1.2 (7.9–9.7)
ND	0.3	0.3	0.3 ± 0.0
ODAO	49.6	58.1	55.7 ± 15.3 (44.9–66.6)
ODW	3.2	3.8	3.6 ± 0.5 (3.3–4.0)
SL	1.5	2.1	1.7 ± 0.1 (1.7–1.8)
SND	1.2	1.9	1.6 ± 0.3 (1.4–1.8)
SPD	5.2	5.8	6.1 ± 0.6 (5.6–6.5)
SSD	8.6	11.7	10.9 ± 1.2 (10.1–11.8)
TaL	20.9	30.8	28.1 ± 3.1 (25.8–30.3)
TL	34.6	48.3	45.1 ± 4.9 (41.6–48.5)
TMH	3.1	4.4	4.0 ± 0.5 (3.6–4.4)
TMW	3.2	5.3	4.7 ± 1.2 (3.8–5.5)
VFH	2.2	2.5	2.5 ± 0.4 (2.2–2.7)
VTL	1.2	2.6	1.8 ± 0.6 (1.3–2.2)

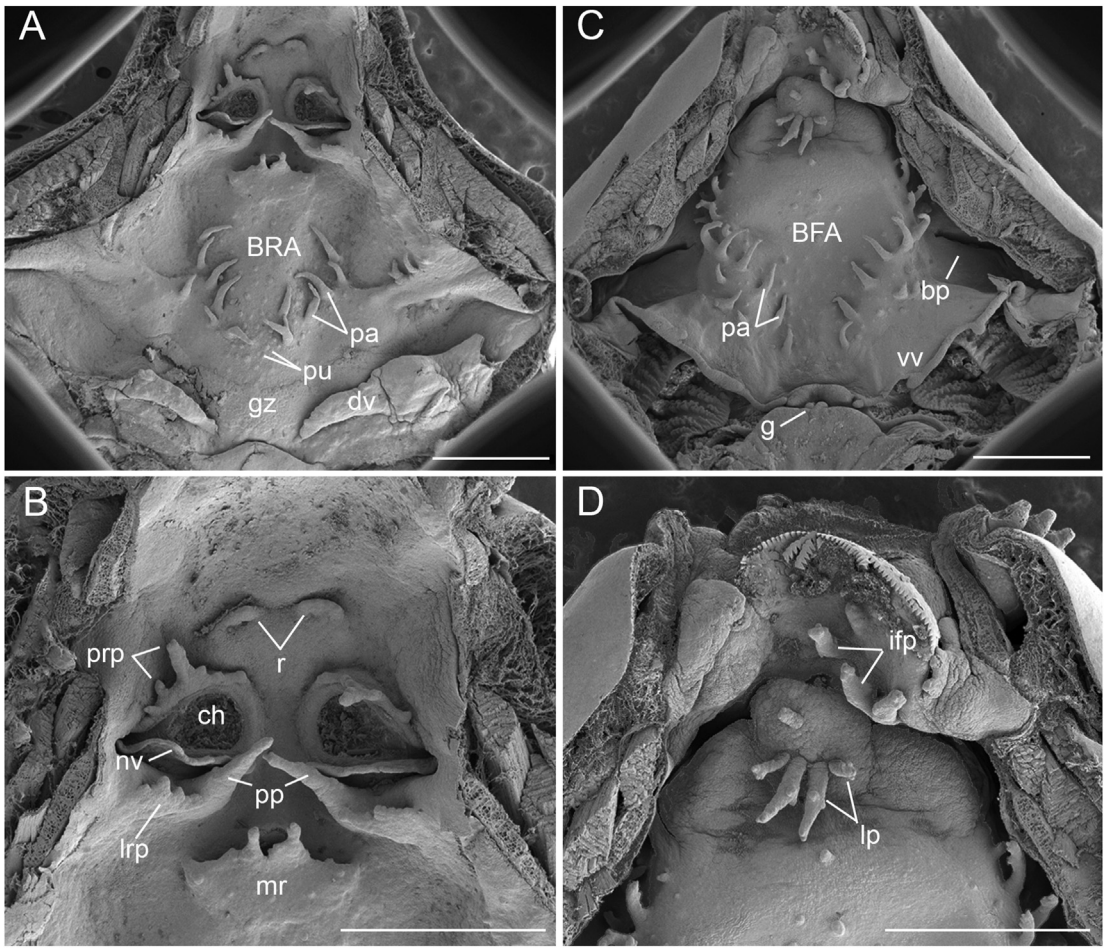

Fig. 2. Scanning electron photomicrographs of the buccal roof (A, B) and floor (C, D) of *Lithodytes lineatus* tadpole (stage 40; QCAZ 9530). The region of the infralabial papillae in this specimen was damaged, see the next figure for a correct visualization of this region. BFA = buccal floor arena, bp = buccal pockets, BRA = buccal roof arena, ch = choana, dv = dorsal velum, g = glottis, gz = glandular zone, ifp = infralabial papillae, lp = lingual papillae, lrp = lateral ridge papillae, mr = median ridge, nv = narial valve, pa = papillae, pp = postnarial papillae, prp = prenarial papillae, pu = pustules, r = ridges, vv = ventral velum (scale bar = 1 mm).

BFA with a pustulated anterior edge; second row formed by 3–5 smaller papillae arranged obliquely on each side and posterolaterally to the first row; about 40 pustules found along the BFA midline, few additional pustules arranged laterally and posteriorly outside the BFA. Buccal pockets transversally oriented, width of each of them about 20% of buccal floor width, with elongated and narrow slits, 2–3 pre-pocket papillae. Ventral velum length equivalent to 16% of the buccal roof length, posterior margin scalloped, with about six distinct small peaks over filter cavities, peaks 4% of buccal roof length, and two digitiform projection medially; median notch evident and projecting dorsally. Secretory pits visible only on median notch. Spicular support conspicuous; spicular length about 15% of buccal floor length. Glottis partially visible.

3.3. Skeleton (stage 39)

Chondrocranium total length is 12 mm; overall elliptical/rectangular in dorsal view, longer than wide (CMW/CTL = 0.55), and depressed in lateral view (CMH/CMW = 0.38), highest at the level of the *processus muscularis quadrati* and widest at posterior portion of palatoquadrate (Fig. 4A and B).

Neurocranium. Ethmoidal region: *cartilago suprarostralis* arc-shaped in dorsal view. Corpus and ala extensively fused forming a massive flat and wide structure; corpus projects anteriorly beyond the plane of articulation between the suprarostral and the *cornua trabeculae*; alae curving posteriorly, ending in a dorsolateral *processus posterior dorsalis*. A small *processus anterior dorsalis* appears as a medial projection on the dorsomedial margin of the ala (Fig. 4C); no adrostral tissue.

The *cornua trabeculae* extend anteriorly from the *planum trabecularum anticum*, diverging distally forming a V in dorsal view, the initial portion flexing upwards and then slightly downwards in lateral view, representing 15% of total chondrocranial length. Each *cornu* almost of uniform width throughout its length, anterior margin straight with a small pointed lateral process; the *cornu* articulates with the suprarostral ala. *Processus lateralis trabeculae* protrudes ventrolaterally in the middle third of each *cornu*. *Planum trabecularum anticum* wider than long (PTAW/PTAL = 3.33). *Tectum nasi* bears a *foramen orbitonasalis* and a slight *lamina orbitonasalis*.

Orbitotemporal region: the *foramina craniopalatina* and *foramina carotica primaria* are visible on the cranial floor. Orbital cartilages slightly chondrified; *foramen opticum* and the *foramen oculomotorium* of similar diameter and a largest and crescent moon shape *foramen prooticum* is located between the otic capsule and the orbital cartilage. Frontoparietal fontanelle bell-shaped and delimited laterally by a thin *taenia tecti marginalis* and posteriorly by a *tectum synoticum* which is about 10% of the chondrocranium length.

Otooccipital region: otic capsules overall quadrangular (OCW/OCL = 0.87; OCH/OCW = 0.93), corresponding to approximately 20% of total chondrocranial length. A *crista parotica* protrudes

Fig. 3. Detail of the buccal floor of *Lithodytes lineatus* tadpole (stage 40; QCAZ 25190). The asterisks indicate the infralabial papillae (scale bar = 0.5 mm).

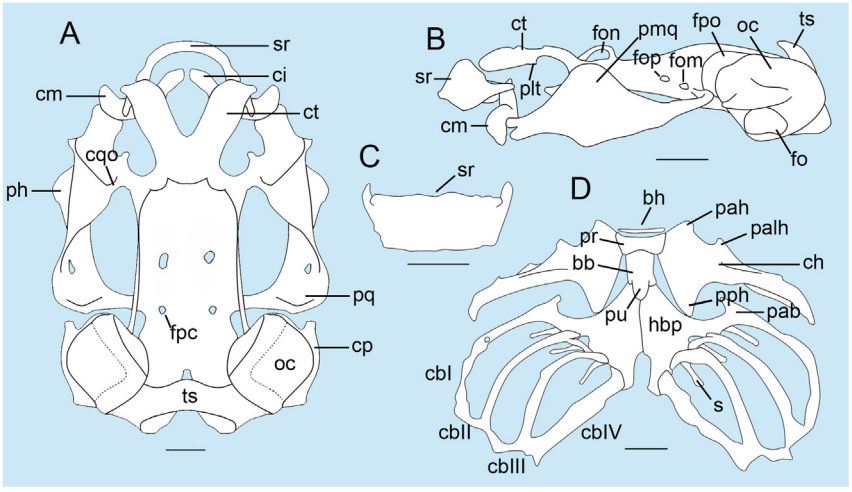

Fig. 4. Skeleton of *Lithodytes lineatus* tadpole at stage 39 (QCAZ 29257). Chondrocranium in (A) dorsal and (B) lateral views, (C) *cartilago suprarostralis* in frontal view, and (D) hyobranchial apparatus in ventral view. Ossifications are not shown. Bb = basibranchial, bh = basihyal, cbI–cbIV = ceratobranchial I–IV, ch = ceratohyal, ci = *cartilago infrarostralis*, cm = *cartilago meckeli*, cp = *crista parotica*, cqo = *commissura quadratoorbitalis*, ct = *cornua trabeculae*, fo = *fenestra ovalis*, fom = *foramen oculomotorium*, fon = *foramen orbitonasalis*, fop = *foramen opticum*, fpc = *foramen caroticum primarium*, fpo = *foramen prooticum*, hbp = hypobranchial plate, oc = otic capsule, pab = *processus anterior branchialis*, pah = *processus anterior hyalis*, palh = *processus anterolateralis hyalis*, ph = *processus hyoquadrati*, plt = *processus lateralis trabeculae*, pmq = *processus muscularis quadrati*, pph = *processus posterior hyalis*, pq = *palatoquadrate*, pr = *pars reuniens*, pu = *processus urobranchialis*, s = spicule, sr = *cartilago suprarostralis*, ts = *tectum sinoticum* (scale bar = 1 mm).

horizontally from the lateral walls of the otic capsules. Each crista bears an anterior and conical anterolateral process and a posterior and small triangular posterolateral process. An ovoid *fenestra ovalis*, about 10% of chondrocranial total length, is distinct below the crista parotica. The *arcus occipitalis* extends posteromedially from the basal plate towards the otic capsules, bearing the occipital condyles and forming the medial and ventral margins of the *foramen jugulare*. A *foramen perilymphaticum inferior* is also found on the ventromedial surface of the otic capsules. A notochordal notch is distinct on the basal plate and represents about 10% of total chondrocranial length.

Visceral components. Palatoquadrate: Palatoquadrate slightly expanded posteriorly; the lateral margin has a concave contour in dorsal view and the posterolateral margin curves slightly upwards to connect with the orbital cartilage via the *processus ascendens*; the lateral margin of the subocular arc is smooth. *Processus ascendens* rod-like, forming a right angle relative to the main axis of the body and curving dorsomedially to attach to the orbital cartilage almost at

the level of the *foramen oculomotorium* (“intermediate”condition, Sokol, 1981). The posterior end of the *processus muscularis quadrati* bears an ovoid foramen. The *commissura quadratocranialis anterior* has a small and triangular *processus quadratoethmoidalis* on its anterior margin. *Processus muscularis quadrati* overall triangular, wide, its dorsal edge inclines medially toward the braincase and is continuous with the *processus antorbitalis* through a *commissura quadratoorbitalis*. The *processus hyoquadrati* is found below the muscular process; it is subtriangular and wide. The *pars articularis quadrati* is wider than long (PAQW/PAQL = 1.22), with about 6% of the chondrocranial length.

Cartilago meckeli and cartilago infrarostralis: *Cartilago meckeli* slightly V-shaped in dorsal view, elongated (CML/CMW = 0.42), and arranged at almost 60° angle relative to the main axis of body. *Processus retroarticularis*, *p. dorsomedialis*, and *p. ventromedialis* distinct. *Cartilago infrarostralis* crescent-shaped; its anterior margin curved outwardly and connect each other medially, forming a slightly open V-shape structure in dorsal view, wider than long (CIW/CIL = 0.70).

Hyobranchial apparatus (Fig. 4D): *Ceratohyalia* medially flat and oriented perpendicular to main body axis; articular condyle stout and extends laterodorsally from its anterior margin. *Processus anterior hyalis* and *processus anterolateralis hyalis* triangular, with *p. anterior hyalis* larger (PAlHL/PAHL = 0.65). *Processus posterior hyalis* triangular and well-developed. Basihyal elongated, thin, and barely visible. *Pars reuniens* overall rectangular and slightly chondrified; wider than long, with posterior edge bearing a distinct notch. Basibranchial elongated, with a distinct *processus urobranchialis*, articulating with the branchial baskets. Hypobranchial plates triangular-shaped and articulate medially by a synchondrosis; their posterior edges diverge forming an inverted U-shaped. Branchial baskets formed by four *ceratobranchialia* distally joined by terminal commissurae; *ceratobranchialia* lack lateral projections. Ceratobranchial I continuous with the hypobranchial plates through a strip of cartilage which bears a triangular and medially inclined *processus anterior branchialis*, while *ceratobranchialia* II, III, and IV are fused to it. *Ceratobranchialia* II and III with an ‘open’ *processus branchialis*. Spicules project dorsally from *ceratobranchialia* I, II, and III at the point of attachment with the hypobranchial plates.

Measurements (in mm, except CMA and CIA which are in degrees). CTL = 12.0, CMW = 6.6, CMH = 2.5, CTrL = 1.8, OCL = 2.5, OCW = 2.2, OCH = 2.0, PTrL = 0.5, PTrW = 1.6, CTMW = 1.1, PAQL = 0.7, PAQW = 0.9, CML = 0.9, CMW = 2.1, CIL = 0.6, CIW = 0.8, CMA = 6.1, CIA = 98, PAHL = 0.6, PAlHL = 0.4.

4. Discussion

Previous work on the tadpole of *L. lineatus* compared aspects of normal and abnormal larval development and mentioned features of the morphology of captive-raised larvae from Fundo Flor, Peru (Regös & Schlüter, 1984). Subsequently, the tadpole external morphology was described and illustrated based on material collected at Villavicencio, Colombia (Lamar & Wild, 1995) and from captive raised specimens from the Panguana Biological Research Station, Peru (Schlüter & Regös, 1996). These previous reports are overall similar to the larvae we examined from Ecuador. In our material, the oral disc has a distinct midventral pleat on labium not described before; however, the illustration of the oral disc of Lamar & Wild (1995) shows an evident deep midventral emargination. Moreover, the description of Schlüter & Regös (1996) was based on a Gosner stage 25 specimen. Larval characters can be highly variable in early stages of development (Grosjean, 2005); consequently, differences among the reports may be related to ontogenetic differences.

Even considering our limited sample size, previous works on *L. lineatus* larvae reported markedly larger tadpoles (TL) than in our sample: TL = 43.0 mm in stage 33 specimens (n = 2; Lamar & Wild, 1995) vs. TL = 34.6 mm at stage 33 (this work) and for a stage 25 larva of Schlüter & Regös (1996). Phenotypic plasticity of larval morphometrics and growth rate has been reported for intra- and interpopulation levels and may be ecological dependent, e.g., diet, temperature, habitat, and interactions with environment (Pearman, 1993; Van Buskirk, 2002; McIntyre et al., 2004). However, we cannot discard that *L. lineatus* may represent more than one taxonomic entity, since genetic divergences among populations of this species were described (Fouquet et al., 2007; de Sá et al., 2014), and the species has also been reported to have populations with disjunct distributions (Barrio-Amorós et al., 2019).

Variation in LTRF among *L. lineatus* samples was also reported (Lamar and Wild, 1995), with most individuals presenting absence of anterior tooth rows: LTRF 0/1 or 0/2 (stages 31, 32, and 34), 0/3 (stage 37, 40), 0/0 (stages 36, 38), and a single specimen with the standard LTRF 2(2)/3(1) (stage 37), as well as specimens entirely lacking keratinized jaw sheaths. These authors stated that “an ontogenetic pattern can be deciphered if one assumes that rows are added progressively with age”. However, this is unlikely due to the apparent lack of a logical sequence of emergence and disappearance of the rows (e.g., LTRF 0/3 in stage 37 and 40 and 0/0 in stages 36 and 38) contradicting the order of appearance known for most anuran species (Thibaudeau & Altig, 1988). Moreover, our sampling has a LTRF 2(2)/3(1) at stages 33, 39, and 40 as well as the reported specimen at stage 25 from Schlüter & Regös (1996). Likely Lamar and Wild’s report may correspond to an abnormal individual or population, that show a very similar pattern of abnormalities found in larvae subject to endocrine disruption (Fabrezi et al., 2019), which can be caused by use of pesticides and herbicides that wash into freshwater environments (de Sá, 2005).

Tadpoles are known for more than half of the currently known Leptodactylinae species; *Hydrolaetare* is the only genus for which tadpoles remain unknown. Nevertheless, most larval descriptions of the subfamily are restricted to external morphology and information on internal morphology is available for about 20% of the species (see supplementary materials SM.02–04). Larval traits, primarily for *Leptodactylus,* the largest and best-known genus in the subfamily, have been used with relative success in systematics and taxonomy (Larson & de Sá, 1998; Miranda et al., 2014; Grosso, 2015; Mello et al., 2018).

The tadpoles of Leptodactylinae have a potentially important variability, range from species with generalized morphology, as in larvae of *Leptodactylus* species of the *fuscus* group and in *Adenomera* species with exotrophic larvae (Sazima & Bokermann, 1978; Carvalho & Giaretta, 2013; Zaracho & Kokubum, 2017), to tadpole with highly specialized morphology, as the *Adenomera* species with endotrophic tadpoles (Heyer & Silverstone, 1969; Kokubum & Giaretta, 2005; Menin et al., 2009), which reflects the diversity of reproductive modes present in the subfamily (de Sá et al., 2014; Pereira et al., 2015). Despite the overall larval morphology of *L. lineatus* seems to be generalized, there are some particularities that will be discussed later. Currently, the main larval features common to Leptodactylinae, including *Lithodytes*, but not necessarily exclusive to them, are (i) the eyes positioned dorsally (except in some *Adenomera*), (ii) oral disc without lateral emarginations (with rare exceptions, e.g., *Leptodactylus elenae* Heyer, 1978), (iii) LTRF 2[2]/3[1] (except in some *Leptodactylus* of *pentadactylus* group and some *Adenomera*), (iv) vent tube medial, (v) presence of a pair of postnarial papillae, (vi) secretory pits visible only on the margins of dorsal velum, (vii) *processus pseudopterygoideus* absent, (viii) *commissura quadratoorbitalis* present, and (viiii) an “intermediate” attachment of the *processus ascendens* to the braincase (except in

some *Leptodactylus* of *melanonotus* group; see supplementary materials SM.02–04). On the other hand, some distinct traits could be useful to differentiate *Lithodytes*, hence supporting the taxonomic validity of the genus (de Sá et al., 2014). For example, the marginal papillae row lacking ventromedial gap and the presence of labial tooth rows readily distinguishes *Lithodytes* from the endotrophic tadpoles of its sister clade *Adenomera* [*A.* aff. *hylaedactyla*, *A. andreae* (Müller, 1923), *A. hylaedactyla* (Cope, 1868), *A. marmorata* Steindachner, 1867, and *Adenomera* sp.; Hero, 1990; Heyer et al., 1990; Kokubum et al., 2008; Menin et al., 2009; FACN pers. obs.]. Moreover, the following traits seem autapomorphic within Leptodactylinae: (i) suprarostral corpus and ala fused into a large flat and wide structure, (ii) presence of three pair of infralabial papillae, (iii) presence of prenarial papillae, with the most lateral one three times longer than other papillae, and (iv) a broad and pocket-like shaped median ridge (supplementary materials SM.03–04). Additionally, *L. lineatus* larvae have an overall elliptical/rectangular body reflecting its chondrocranial anatomy (i.e., palatoquadrate only slightly expanded posteriorly and a rectangular braincase) that readily distinguishes it from *Adenomera* and *Leptodactylus* tadpoles (palatoquadrate and cranial floor expanded posteriorly; supplementary materials SM.04).

The choanae of *L. lineatus* are drop-shaped, clearly distinct from the slit-shaped internal choanae of most Leptodactylidae species (Nascimento et al., 2020; supplementary materials SM.03). Furthermore, in *Lithodytes* the choanae are formed by a narial opening itself (perforated section) and by a concavity, i.e., a non-perforated, anteromedial section. This same structure was reported for some Hylidae (Magalhães et al., 2015; d'Heursel & Haddad, 2007) and Centronelidae (Dias et al., 2020), suggested as independent synapomorphies for the latter family and for the hylid subfamily Cophomantinae (Kolenc et al., 2008; Dias et al., 2020). These concavities originally were defined as vacuities (Wassersug, 1980), and later the term was restricted to only the round-shaped concavities of Cophomantinae (Kolenc et al., 2008) to differentiate them from the oval-shaped concavities found in other hylids (e.g., *Scinax* Wagler, 1830 and *Pseudis* Wagler, 1830; Conte et al., 2007; Kolenc et al., 2008). Nonetheless its variety of shapes (Fig. 5), all of them are lining by a ciliated or microvillied epithelium that secretes mucous, which have been suggested to have a chemoreceptive function (Wassersug, 1980; Kolenc et al., 2008). We observed these concavities in other Leptodactylinae, e.g., some *Adenomera* (i.e., exotrophic tadpole of *A. thomei*) and in species of the *L. pentadactylus* species group (*sensu* de Sá et al., 2014), e.g., *L. labyrinthicus*, *L. pentadactylus*, and *L. vastus* (Fig. 6K). We also clearly observed it in illustrations of previous work, e.g., *Leptodactylus knudseni* Heyer, 1972 and *L. labyrinthicus* tadpoles (Wassersug and Heyer, 1988; (Miranda and Ferreira, 2008)). Further studies are needed to ascertain the distribution of this trait in other lineages and to test its functional meaning.

Interestingly, some other features of *L. lineatus* tadpoles also occur independently in some species of the *L. pentadactylus* species group, such as (i) a long muscular tail, (ii) the oral disc positioned almost terminally (Fig. 6A–C), (iii) a comparatively shorter and wider *cornua trabeculae*, (iv) the suprarostral components extensively fused (Hero, 1990; Heyer, 1970; Larson & de Sá, 1998; Vieira et al., 2007; Menin et al., 2010; FACN pers. obs.), (v) the marginal papillae comparatively larger and in a less number on the oral disc (~6 papillae/mm against ~10–20 papillae/mm in remaining species; Fig. 6D–F), and (vi) a midventral pleat on labium of the oral disc (Fig. 6G–I). When we transform these traits into character-states and optimize on the available Leptodactylinae phylogeny (de Sá et al., 2014; Fouquet et al., 2014), a pattern of possible convergence emerges between *Lithodytes* and some species of the *L. pentadactylus* group, showing an apparent strong evolutionary correlation among them (Fig. 7). Most character-states of *Lithodytes* are homoplastic with those of a subclade of the *L. pentadactylus* group (i.e., *L. fallax* Müller, 1923, *L. knudseni*, *L. labyrinthicus*, *L. myersi* Heyer, 1995, *L. paraensis* Heyer, 2005, *L. pentadactylus*, *L. peritoaktites* Heyer, 2005, *L. savagei* Heyer, 2005, and *L. vastus*). At least three of these states (almost terminally oral disc, *cornua trabeculae* short and wide, and suprarostral components fused) have been related to carnivore diet (Heyer, 1975, 2005), which was previously reported for some species of this *Leptodactylus* subclade (Cardoso & Sazima, 1977; Heyer & Heyer, 2006; Silva et al., 2005; Rodrigues et al., 2007). Whether the peculiar morphology of *Lithodytes* is also correlated with carnivorous diet is not known since the diet of *Lithodytes* tadpoles remains undetermined. *Lithodytes lineatus* was reported to use leaf-cutter ant nests *(A. cephalotes*) as breeding site (Schlüter & Regös, 1981; Schlüter et al., 2009) and tadpoles were found in water filled depressions at underwater burrows associated with these nests. Intriguingly, most of captive-raised *L. lineatus* tadpoles that were fed with commercial fish food died (Regös and Schlüter, 1984), which suggest that larvae may feed on these ants, eggs and/or other subterranean invertebrates.

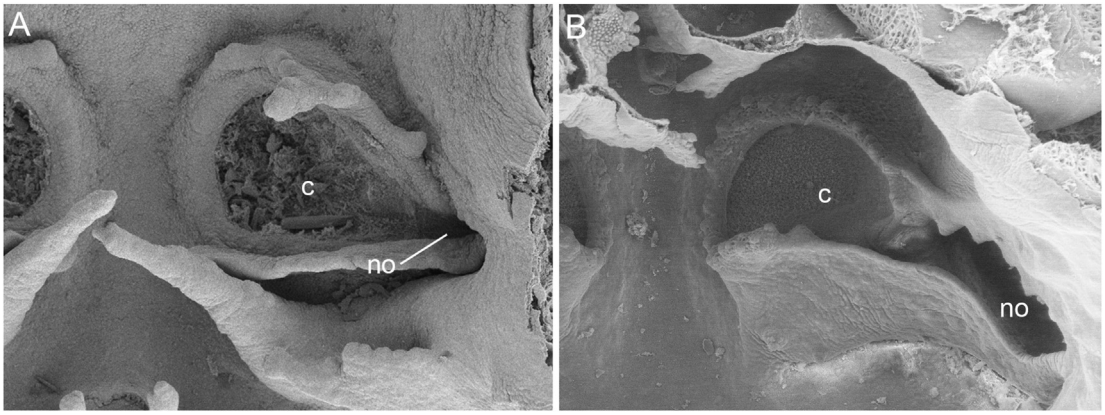

Fig. 5. Detail of the choanae of (A) *Lithodytes lineatus* (Leptodactylidae, stage 40; QCAZ 9530) and (B) *Boana punctata* (Hylidae, stage 34; UFMG 637) tadpoles. Note the difference between these two structures. In *L. lineatus*, the concavity appears as a smooth continuation of the circular narial opening, while in *B. punctata*, there is an internal projection between the concavity and the slit-shaped narial opening itself. C = concavity, no = narial opening (not to scale).

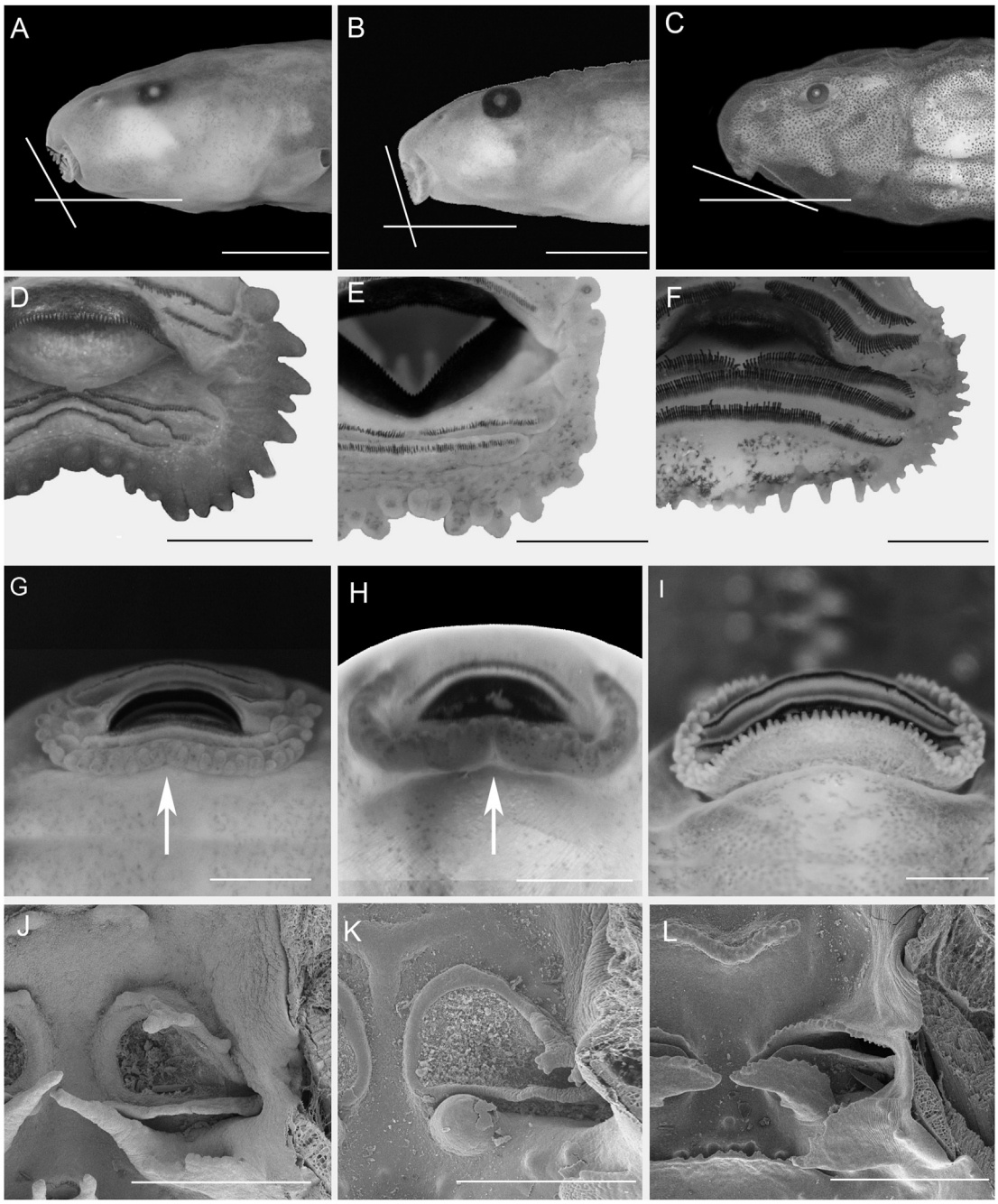

Fig. 6. Comparative larval characters among *Lithodytes lineatus* (stage 33, QCAZ 8334), *Leptodactylus vastus* (member of the *L. pentadactylus* species group, stage 35, MUFAL 10184) and remaining *Leptodactylus*. First row: oral disc orientation in (A) *L. lineatus* (almost terminal), (B) *L. vastus* (almost terminal), and (C) *L. pustulatus* (almost ventral, stage 27, CFBH 9024). Second row: relative size of the marginal papillae in (D) *L. lineatus* (large), (E) *L. vastus* (large), and (F) *L. fuscus* (small, stage 37, AGARDA 9367). Third row: midventral pleat on labium in (G) *L. lineatus* (present), (H) *L. vastus* (present), and (I) *L.* cf. *latrans* (absent, stage 30, UFMG 145). Fourth row: choana shape in (J) *L. lineatus* (drop-shaped), (K) *L. vastus* (drop-shaped), and (L) *L. troglodytes* (slit-shaped, stage 36, AGARDA 9365).

Analyses of evolutionary morphology of tadpoles relative to episodes of anuran lineage diversification suggested that younger clades may have expanded their morphological diversity through repeated convergence, i.e., homoplasy, into similar morphospaces (Roelants et al., 2011). Similar conclusions were drawn in Australian frogs (Sherratt et al., 2017). The putative homoplasies between *Lithodytes* and a subclade of the *L. pentadactylus* group may be convergent adaptations to morpho-functional constraints. Nevertheless, these putative homoplastic and autapomorphic characters serve as diagnostic traits for *Lithodytes*, corroborating its recognition as a distinct genus within Leptodactylidae and reinforcing the role and contribution of larval characters for understanding the evolution and systematics of anurans (Larson & de Sá, 1998; Maglia et al., 2001; Larson, 2005; Vera Candioti, 2007).

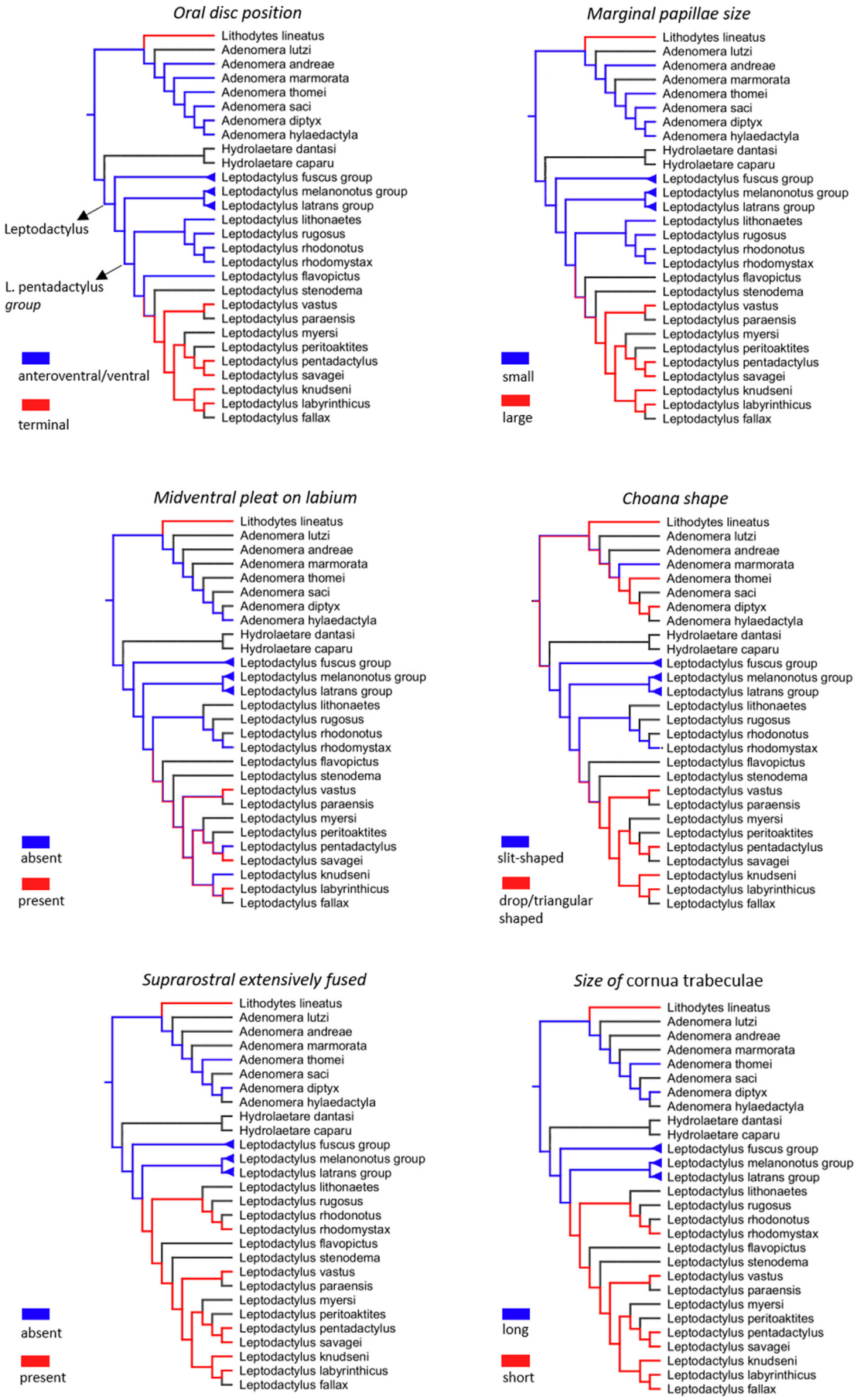

Fig. 7. Optimization of some larval characters on the topology of the subfamily Leptodactylinae (from de Sá et al., 2014, except the intrageneric relationships of *Adenomera*, which follows Fouquet et al., 2014). Branches colored in black are those for which the character is unknown for the respective taxa.

Declaration of competing interest

The authors declare that they have no known competing financial interests or personal relationships that could have appeared to influence the work reported in this paper.

Acknowledgements

We thank Santiago Ron (QCAZ) for loan of the specimens, Tiago Pezzuti for the photomicrograph of *Boana punctata* and two anonymous reviewers for their helpful comments that greatly improved the manuscript. We are also grateful to Center of Microscopy at the Universidade Federal de Minas Gerais for providing the equipment and technical support for analysis involving electron microscopy (www.microscopia.ufmg.br). Paulo C. A. Garcia acknowledges support by the Conselho Nacional de Desenvolvimento Científico e Tecnológico (CNPq) Brazil. This work is part of the Doctoral thesis of the first author and partially financed by the Coordenação de Aperfeiçoamento de Pessoal de Nível Superior (CAPES), Brazil (Finance Code 001).

Appendix A. Supplementary data

Supplementary data to this article can be found online at https://doi.org/10.1016/j.jcz.2020.12.003.

References

Alcalde, L., Rosset, S.D., 2003. Descripción y comparación del condrocráneo en larvas de *Hyla raniceps* (Cope, 1862), *Scinax granulatus* (Peters, 1871) y *Scinax squalirostris* (A. Lutz, 1925) (Anura: Hylidae). Cuad. Herpetol. 17, 33–49.

Alcalde, L., Vera Candioti, F., Kolenc, F., Borteiro, C., Baldo, D., 2011. Cranial anatomy of tadpoles of five species of *Scinax* (Hylidae, Hylinae). Zootaxa 2787, 19–36. https://doi.org/10.11646/zootaxa.2787.1.2.

Almeida, A.P., Ângulo, A., 2006. A new species of *Leptodactylus* (Anura: Leptodactylidae) from the state of Espírito Santo, Brazil, with remarks on the systematics of associated populations. Zootaxa 1334, 1–25. https://doi.org/10.11646/zootaxa.1334.1.1.

Altig, R., Johnston, G.F., 1989. Guilds of anuran larvae: relationships among developmental modes, morphologies, and habits. Herpetol. Monogr. 3, 81–109. https://doi.org/10.2307/1466987.

Altig, R., McDiarmid, R.W., 1999. Body plan: development and morphology. In: McDiarmid, R.W., Altig, R., Eeds (Eds.), Tadpoles: the Biology of Anuran Larvae. University of Chicago Press, Chicago and London, pp. 24–51.

Andrade, E.B., Ferreira, J.S., Takazone, A.M., Libório, A.E.C., Weber, L.N., 2018. Description of the tadpole of *Pseudopaludicola canga* Giaretta and Kokubum, 2003 (Anura: Leptodactylidae). S. Am. J. Herpetol. 13, 64–72. https://doi.org/10.2994/SAJH-D-17-00032.1.

Barrio-Amorós, C.L., Rojas-Runjaic, F.J.M., Señaris, J.C., 2019. Catalogue of the amphibians of Venezuela: illustrated and annotated species list, distribution, and conservation. Amphib. Reptile Conserv. 13, 1–198.

Bell, B.D., Wassersug, R.J., 2003. Anatomical features of *Leiopelma* embryos and larvae: implications for anuran evolution. J. Morphol. 256, 160–170. https://doi.org/10.1002/jmor.10082.

Boulenger, G.A., 1884. "1883". On a collection of frogs from Yurimaguas, Huallaga river, Northern Peru. Proc. Zool. Soc. Lond. 1883 635–638.

Cannatella, D., 1999. Architecture: cranial and axial musculoskeleton. In: McDiarmid, R. W., Altig, R. (Eds.), Tadpoles: the Biology of Anuran Larvae. University of Chicago Press, Chicago and London, In: McDiarmid RW, Altig R (eds) Tadpoles: the biology of anuran larvae. University of Chicago Press, Chicago, pp. 52–91.

Cardoso, A.J.A., Sazima, I., 1977. Batracofagia na fase adulta e larvária da rã-pimenta, *Leptodactylus labyrinthicus* (Spix, 1824) Anura. Leptodactylidae. Ciênc. Cult. 29, 1130–1132.

Carvalho, T.R., Giaretta, A.A., 2013. Taxonomic circumscription of *Adenomera martinezi* (Bokermann, 1956) (Anura: Leptodactylidae: Leptodactylinae) with the recognition of a new cryptic taxon through a bioacoustic approach. Zootaxa 3701, 207–237. https://doi.org/10.11646/zootaxa.3701.2.5.

Ceron, K., Santana, D.J., 2017. The tadpole of *Physalaemus nanus* (Boulenger, 1888) (Anura, Leptodactylidae) from southern Brazil. Zootaxa 4277, 280–284. https://doi.org/10.11646/zootaxa.4277.2.9.

Conte, C.E., Nomura, F., Rossa-Feres, D.C., d'Heursel, A., Haddad, C.F.B., 2007. The tadpole of *Scinax catharinae* (Anura: Hylidae) with description of the internal oral morphology, and a review of the tadpoles from the *Scinax catharinae* group. Amphib-Reptilia 28, 177–192. https://doi.org/10.1163/156853807780202387.

Cope, E.D., 1868. An examination of the Reptilia and Batrachia obtained by the Orton expedition to equador and the upper Amazon, with notes on other species. Proc. Acad. Nat. Sci. Phila. 20, 96–140.

d'Heursel, A., Haddad, C.F.B., 2007. Anatomy of the oral cavity of Hylid larvae from the genera *Aplastodiscus, Bokermannohyla*, and *Hypsiboas* (Amphibia, Anura): description and systematic implications. J. Herpetol. 41, 458–468. https://doi.org/10.1670/0022-1511(2007)41[458:AOTOCO]2.0.CO;2.

de Sá, R.O., 2005. Global Biodiversity Crisis: genetic diversity and amphibian extinction. Agrociencia IX (1–2), 513–522.

de Sá, R.O., Grant, T., Camargo, A., Heyer, W.R., Ponssa, M.L., Stanley, E., 2014. Systematics of the neotropical genus *Leptodactylus* Fitzinger, 1826 (Anura: Leptodactylidae): phylogeny, the relevance of non-molecular evidence, and species accounts. S. Am. J. Herpetol. 9, 1–100. https://doi.org/10.2994/SAJH-D-13-00022.1.

Dias, P.H., Anganoy-Criollo, M., Rada, M., Grant, T., 2020. Comparative larval buccopharyngeal morphology of two glass frog species (Anura: Centrolenidae: Vitreorana). Zool. Anz. 289, 118–122. https://doi.org/10.1016/j.jcz.2020.10.007.

Dias, P.H., Araujo-Vieira, K., Santos, R.F., Both, C., 2019. Review of the internal larval anatomy of the *Proceratophrys bigibbosa* species Group (Anura: Odontophrynidae), with description of the tadpole of *P. brauni* Kwet and Faivovich, 2001. Copeia 107, 417–429. https://doi.org/10.1643/CH-18-138.

Dingerkus, G., Uhler, L.D., 1977. Enzyme clearing of alcian blue stained whole small vertebrates for demonstration of cartilage. Stain Technol. 52, 229–232. https://doi.org/10.3109/10520297709116780.

Duellman, W.E., 2005. Cusco Amazónico: the Lives of Amphibians and Reptiles in an Amazonian Rainforest. Comstock, Ithaca.

Fabrezi, M., Lozano, V.L., Cruz, J.C., 2019. Differences in responsiveness and sensitivity to exogenous disruptors of the thyroid gland in three anuran species. J. Exp. Zool. Part. B 332, 279–293. https://doi.org/10.1002/jez.b.22908.

Fitzinger, L.J.F.J., 1826. Neue Classification der Reptilien nach ihren Natürlichen Verwandtschaften nebst einer Verwandtschafts-Tafel und einem Verzeichnisse der Reptilien-Sammlung des K. K. Zoologisch Museum's zu Wien. J. G. Heubner, Wien.

Fitzinger, L.J.F.J., 1843. Systema Reptilium. Fasciculus Primus. Braumüller et Seidel, Wien.

Fouquet, A., Blotto, B.L., Maronna, M.M., Verdade, V.K., Junca, F.A., de Sá, R.O., Rodrigues, M.T., 2013. Unexpected phylogenetic positions of the genera *Rupirana* and *Crossodactylodes* reveal insights into the biogeography and reproductive evolution of leptodactylid frogs. Mol. Phylogenet. Evol. 67, 445–457. https://doi.org/10.1016/j.ympev.2013.02.009.

Fouquet, A., Cassini, C.S., Haddad, C.F.B., Pech, N., Rodrigues, M.T., 2014. Species delimitation, patterns of diversification and historical biogeography of the Neotropical frog genus *Adenomera* (Anura, Leptodactylidae). J. Biogeogr. 41, 855–870. https://doi.org/10.1111/jbi.12250.

Fouquet, A., Gilles, A., Vences, M., Marty, C., Blanc, M., Gemmell, N.J., 2007. Underestimation of species richness in neotropical frogs revealed by mtDNA analyses. PLoS One 10, 1–10. https://doi.org/10.1371/journal.pone.0001109.

Frost, D.R., 2020. Amphibian Species of the World: an Online Reference. American Museum of Natural History, New York, USA. Version 6.0 (21th June, 2020). Electronic Database accessible at. http://research.amnh.org/herpetology/amphibia/index.html.

Frost, D.R., Grant, T., Faivovich, J., Bain, R.H., Haas, A., Haddad, C.F.B., de Sá, R.O., Channing, A., Wilkinson, M., Donnellan, S.C., Raxworthy, C.J., Campbell, J.A., Blotto, B.L., Moler, P., Drewes, R.C., Nussbaum, R.A., Lynch, J.D., Green, D.M., Wheeler, W.C., 2006. The amphibian tree of life. Bull. Am. Mus. Nat. Hist. 297, 1–370. https://doi.org/10.1206/0003-0090(2006)297[0001:TATOL]2.0.CO;2.

Gallardo, J.M., 1963. *Hydrolaetare*, nuevo genero de Leptodactylidae (Amphibia) neotropical. Neotropica 9, 42–48.

Gosner, K.L., 1960. A simplified table for staging anuran embryos and larvae with notes on identification. Herpetologica 16, 183–190.

Grosjean, S., 2005. The choice of external morphological characters and developmental stages for tadpole-based anuran taxonomy: a case study in *Rana* (*Sylvirana*) *nigrovittata* (Blyth, 1855) (Amphibia, Anura, Ranidae). Contrib. Zool. 74, 61–76. https://doi.org/10.1163/18759866-0740102005.

Grosso, J.R., 2015. Tadpole morphology of *Leptodactylus plaumanni* (Anura: Leptodactylidae), with comments on the phylogenetic significance of larval characters in *Leptodactylus*. Cuad. Herpetol. 29, 117–129.

Grosso, J.R., Pereyra, M.O., Candioti, F.V., Maciel, N.M., Baldo, D., 2020. Tadpoles of three species of the *Rhinella granulosa* group with a Reinterpretation of larval characters. South. Am. J. Herpetol. 2020 75–84.

Haas, A., 2003. Phylogeny of frogs as inferred from primarily larval characters (Amphibia, Anura). Cladistics 19, 23–89. https://doi.org/10.1016/S0748-3007(03)00006-9.

Hero, J.M., 1990. An illustrated key to tadpoles occurring in the Central Amazon rainforest, Manaus, Amazonas, Brasil. Amazoniana 11, 201–262.

Heyer, W.R., 1970. Studies on the genus *Leptodactylus* (Amphibia: Leptodactylidae). II. Diagnosis and distribution of the *Leptodactylus* of Costa Rica. Rev. Biol. Trop. 16, 171–205.

Heyer, W.R., 1972. The status of *Leptodactylus pumilio* Boulenger (Amphibia, Leptodactylidae) and the description of a new species of *Leptodactylus* from Ecuador. Contrib. Sci. (Los Angel.) 231, 1–8.

Heyer, W.R., 1975. A preliminary analysis of the intergeneric relationships of the frog family Leptodactylidae. Smithsonian Contrib. Zool. 199, 1–55. https://doi.org/10.5479/si.00810282.199.

Heyer, W.R., 1978. Systematics of the *fuscus* group of the frog genus *Leptodactylus* (Amphibia, Leptodactylidae). Science bulletin (Los Angeles, Calif.) 29, 1–85.
Heyer, W.R., 1995. South American rocky habitat *Leptodactylus* (Amphibia: Anura: Leptodactylidae) with description of two new species. Proc. Biol. Soc. Wash. 108, 695–716.
Heyer, W.R., 1998. The relationships of *Leptodactylus diedrus* (Anura, Leptodactylidae). Alytes 16, 1–24.
Heyer, W.R., 2005. Variation and taxonomic clarification of the large species of the *Leptodactylus pentadactylus* species group (Amphibia: Leptodactylidae) from Middle America, Northern South America, and Amazonia. Arq. Zool. (Sao Paulo) 37, 1–86. https://doi.org/10.11606/issn.2176-7793.v37i3p269-348.
Heyer, W.R., Heyer, M.M., 2006. Leptodactylus knudseni. Cat. Am. Amphib. Reptil. 807, 1–12.
Heyer, W.R., Rand, A.S., Gonçalves da Cruz, C.A., Peixoto, O.L., Nelson, C.E., 1990. Frogs of Boracéia. Arq. Zool. (Sao Paulo) 31, 237–410.
Heyer, W.R., Silverstone, P.A., 1969. The larva of the frog *Leptodactylus hylaedactylus* (Leptodactylidae). Fieldiana Zool. 51, 141–145. https://doi.org/10.5962/bhl.title.3047.
Kohler, G., 2012. Color Catalogue for Field Biologist. Herpeton, Offenbach.
Kokubum, M., de Carvalho, N., Sousa, M.B., 2008. Reproductive ecology of *Leptodactylus* aff. *hylaedactylus* (Anura, Leptodactylidae) from an open area in Northern Brazil. S. Am. J. Herpetol. 3, 15–21. https://doi.org/10.2994/1808-9798(2008)3[15:REOLAH]2.0.CO;2.
Kokubum, M.N.C., Giaretta, A.A., 2005. Reproductive ecology and behaviour of a species of *Adenomera* (Anura, Leptodactylinae) with endotrophic tadpoles: systematic implications. J. Nat. Hist. 39, 1745–1758. https://doi.org/10.1080/00222930400021515.
Kolenc, F., Borteiro, C., Alcalde, L., Baldo, D., Cardozo, D., Faivovich, J., 2008. Comparative larval morphology of eight species of *Hypsiboas* Wagler (Amphibia, Anura, Hylidae) from Argentina and Uruguay, with a review of the larvae of this genus. Zootaxa 1927 1–66. https://doi.org/10.11646/zootaxa.1927.1.1.
Lamar, W.W., Wild, E.R., 1995. Comments on the natural history of *Lithodytes lineatus* (Anura: Leptodactylidae), with description of the tadpole. Herpetol. Nat. Hist. 3, 135–142.
Larson, P.M., 2005. Ontogeny, phylogeny, and morphology in anuran larvae: morphometric analysis of cranial development and evolution in *Rana* tadpoles (Anura: Ranidae). J. Morphol. 264, 34–52. https://doi.org/10.1002/jmor.10313.
Larson, P.M., de Sá, R.O., 1998. Chondrocranial morphology of *Leptodactylus* larvae (Leptodactylidae: Leptodactylinae): its utility in phylogenetic reconstruction. J. Morphol. 238, 287–305. https://doi.org/10.1002/(SICI)1097-4687(199812)238:3<287::AID-JMOR2>3.0.CO;2-8.
Laurenti, J.N., 1768. Specimen Medicum, Exhibens Synopsin Reptilium Emendatum cum Experimentis Circa Venena et Antidota Reptilium Austriacorum. Joan. Thom. nob. de Trattnern, Wien.
Lavilla, E.O., Scrocchi, G.J., 1986. Morfometría larval de los géneros de Telmatobiinae (Anura: Leptodactylidae) de Argentina y Chile. Physis 44, 39–43.
Linnaeus, C., 1758. Systema Naturae Per Regna Tria Naturae, Secundum Classes, Ordines, Genera, Species, Cum Characteribus, Differentiis, Synonymis, Locis. Tomus I. Editio decima, reformata, pp. 1–824 [1-4].
Lutz, A., 1930. Segunda memoria sobre especies brasileiras do genero *Leptodactylus*, incluindo outras alliadas/Second paper on Brasilian and some closely related species of the genus *Leptodactylus*. Mem. Inst. Oswaldo Cruz 23, 1–34.
Lutz, A., 1926. Observações sobre batrachios brasileiros/Observations on brazilian batrachians. Mem. Inst. Oswaldo Cruz 19, 139–174.
Maddison, W.P., Maddison, D.R., 2016. Mesquite: a modular system for evolutionary analysis (ver. 3.20) [Computer software]. www.mesquiteproject.org. (Accessed 8 July 2018). Accessed.
Magalhães, F.M., Mercês, E.A., Santana, D.J., Juncá, F.A., Napoli, M.F., Garda, A.A., 2015. The tadpole of *Bokermannohyla flavopicta* Leite, Pezzuti and Garcia, 2012 and oral cavity anatomy of the tadpole of *B. oxente* Lugli and Haddad, 2006 (Anura: H ylidae). S. Am. J. Herpetol. 10, 211–218. https://doi.org/10.2994/SAJH-D-13-00033.1.
Maglia, A.M., Púgener, L.A., Trueb, L., 2001. Comparative development of anurans: using phylogeny to understand ontogeny. Am. Zool. 41, 538–551. https://doi.org/10.1093/icb/41.3.538.
McIntyre, P.B., Baldwin, S., Flecker, A.S., 2004. Effects of behavioral and morphological plasticity on risk of predation in a Neotropical tadpole. Oecologia 141, 130–138. https://doi.org/10.1007/s00442-004-1652-x.
Mello, C.M., Gonçalves, D.D.S., Solé, M., Rossa-Feres, D.D.C., Conte, C.E., 2018. A comparison of tadpoles of two populations of *Leptodactylus plaumanni* (Anura: Leptodactylidae), with a discussion of *Leptodactylus* tadpole morphology. Stud. Neotrop. Fauna Environ. 53, 233–244. https://doi.org/10.1080/01650521.2018.1492661.
Menin, M., de Almeida, A.P., Kokubum, M.N.C., 2009. Reproductive aspects of *Leptodactytus hylaedactylus* (Anura: Leptodactylidae), a member of the *Leptodactylus marmoratus* species group, with a description of tadpoles and calls. J. Nat. Hist. 43, 2257–2270. https://doi.org/10.1080/00222930903097707.
Menin, M., Lima, A.P., Rodrigues, D.J., 2010. The tadpole of *Leptodactylus pentadactylus* (Anura: Leptodactylidae) from central Amazonia. Zootaxa 2508, 65–68. https://doi.org/10.11646/zootaxa.2508.1.5.
Miranda, N.E.O., Maciel, N.M., Tepedino, K.P., Sebben, A., 2014. Internal larval characters in anuran systematic studies: a phylogenetic hypothesis for *Leptodactylus* (Anura, Leptodactylidae). J. Zool. Syst. Evol. Res. 53, 55–66. https://doi.org/10.1111/jzs.12073.
Miranda, N.E.O., Ferreira, A., 2008. Morfologia bucal interna dos girinos de *Leptodactylus labyrinthicus* Spix, 1824 (Amphibia: Anura: Leptodactylidae). Biota Neotropica 8, 225–230. https://doi.org/10.1590/S1676-06032008000100025.
Miranda-Ribeiro, A., 1926. Notas para servirem ao estudo dos Gymnobatrachios (Anura) brasileiros. Arq. Mus. Nac. 27, 1–227.
Müller, L., 1923. Neue oder seltene Reptilien und Batrachier der zoologischen Sammlung des bayerischen Staates. Zool. Anz. 57, 38–42.
Nascimento, F.A.C., de Sá, R.O., Garcia, P.C.A., 2020. Tadpole of the Amazonia frog *Edalorhina perezi* (Anura: Leptodactylidae) with description of oral internal and chondrocranial morphology. J. Morphol. 1, 12. https://doi.org/10.1002/jmor.21286.
Pearman, P.B., 1993. Effects of habitat size on tadpole populations. Ecology 74, 1982–1991. https://doi.org/10.2307/1940841.
Pereira, E.B., Collevatti, R.G., de Carvalho Kokubum, M.N., de Oliveira Miranda, N.E., Maciel, N.M., 2015. Ancestral reconstruction of reproductive traits shows no tendency toward terrestriality in leptodactyline frogs. BMC (Biomed. Chromatogr.) 15, 91. https://doi.org/10.1186/s12862-015-0365-6.
Peters, W.C.H., 1870. Über neue Amphien (*Hemidactylus, Urosaura, Tropdolepisma, Geophis, Uriechis, Scaphiophis, Hoplocephalus, Rana, Entomoglossus, Cystignathus, Hylodes, Arthroleptis, Phyllobates, Cophomantis*) des Königlich Zoologisch Museum. Monatsberichte der Königlichen Preussische Akademie des Wissenschaften zu Berlin 1870 641–652.
Pinheiro, P.D.P., Pezzuti, T.L., Garcia, P.C., 2012. The tadpole and vocalizations of *Hypsiboas polytaenius* (Cope, 1870) (Anura, Hylidae, Hylinae). S. Am. J. Herpetol. 7, 123–134. https://doi.org/10.2994/057.007.0202.
Púgener, L.A., Maglia, A.M., Trueb, L., 2003. Revisiting the contribution of larval characters to an analysis of phylogenetic relationships of basal anurans. Zool. J. Linn. Soc. 139, 129–155. https://doi.org/10.1046/j.1096-3642.2003.00075.x.
Pyron, A.R., Wiens, J.J., 2011. A large-scale phylogeny of Amphibia including over 2800 species, and a revised classification of extant frogs, salamanders, and caecilians. Mol. Phylogenet. Evol. 61, 543–583. https://doi.org/10.1016/j.ympev.2011.06.012.
Regös, J., Schlüter, A., 1984. Erste Ergebnisse zur Fortpflanzungsbiologie von *Lithodytes lineatus* (Schneider, 1799) (Amphibia: Leptodactylidae). Salamandra 20, 252–261.
Rodrigues, D.J., Menin, M., Lima, A.P., 2007. Redescription of the tadpole of *Leptodactylus rhodomystax* (Anura: Leptodactylidae) with natural history notes. Zootaxa 1509, 61–67. https://doi.org/10.11646/zootaxa.1509.1.6.
Rodrigues, G.D.V., Nascimento, F.A.C., Almeida, J.P.F.A., Mott, T., 2017. The tadpole of *Scinax skuki* (Anura: Hylidae) from the type locality, with a description of its larval skeleton. Stud. Neotrop. Fauna 52, 204–215. https://doi.org/10.1080/01650521.2017.1342485.
Roelants, K., Haas, A., Bossuyt, F., 2011. Anuran radiations and the evolution of tadpole morphospace. Proc. Natl. Acad. Sci. Unit. States Am. 108, 8731–8736. https://doi.org/10.1073/pnas.1100633108.
Sazima, I., Bokermann, W.C.A., 1978. Cinco novas espécies de *Leptodactylus* do centro e sudeste brasileiro (Amphibia, Anura, Leptodactylidae). Rev. Bras. Biol. 38, 899–912.
Schlüter, A., 1980. Bio-akustische Untersuchungen an Leptodactyliden in einem begrenzten Gebiet des tropischen Regenwaldes von Peru (Amphibia: Salientia: Leptodactylidae). Salamandra 16, 227–247.
Schlüter, A., Löttker, P., Mebert, K., 2009. Use of an active nest of the leaf cutter ant *Atta cephalotes* (Hymenoptera: Formicidae) as a breeding site of *Lithodytes lineatus* (Anura: Leptodactylidae). Herpetol. Notes 2, 101–105.
Schlüter, A., Regös, J., 1981. *Lithodytes lineatus* (Schneider, 1799) (Amphibia: Leptodactylidae) as a dweller in nests of the leaf cutting ant *Atta cephalotes* (Linnaeus, 1758) (Hymenoptera: Attini). Amphib-Reptilia 2, 117–121. https://doi.org/10.1163/156853881X00159.
Schlüter, A., Regös, J., 1996. The tadpole of *Lithodytes lineatus* – with note on the frogs resistance to leaf-cutting ants (Amphibia: Leptodactylidae). Stuttgarter Beitr. Naturk. Ser. A 536, 1–4.
Schneider, J.G., 1799. Historia Amphibiorum Naturalis et Literarariae. Fasciculus Primus. Continens Ranas, Calamitas, Bufones, Salamandras et Hydros in Genera et Species Descriptos Notisque suis Distinctos. Friederici Frommanni, Jena.
Sherratt, E., Vidal-Garcia, M., Anstis, M., Keogh, J.S., 2017. Adult frogs and tadpoles have different macroevolutionary patterns across the Australian continent. Nat. Ecol Evol 1, 1385–1391. https://doi.org/10.1038/s41559-017-0268-6.
Silva, W.R., Giaretta, A.A., Facure, K.G., 2005. On the natural history of South American pepper frog, *Leptodactylus labyrinthicus* (Spix, 1824) (Anura: Leptodactylidae). J. Nat. Hist. 39, 555–566. https://doi.org/10.1080/00222930410001671273.
Sokol, O.M., 1981. The larval chondrocranium of *Pelodytes punctatus*, with a review of tadpole chondrocrania. J. Morphol. 169, 161–183. https://doi.org/10.1002/jmor.1051690204.
Spix, J.B., 1824. Animalia nova sive Species novae Testudinum et Ranarum quas in itinere per Brasiliam annis MDCCCXVII–MDCCCXX jussu et auspiciis. Maximiliani. Hübschmann. Monarchii 1–53.
Steffen, G.A., 1815. De Ranis Nonnullis Observationes Anatomicae Quas Consensu Gratiosae Facultatis Medicae. Joannis Friderici Starckii, Berlin.
Steindachner, F., 1867. Reise der österreichischen Fregatte Novara um die Erde in den Jahren 1857, 1858, 1859 unter den Befehlen des Commodore B. von Wüllerstorf-Urbair. Zologischer Theil. 1. Amphibien. K. . K. Hof- und Staatsdruckerei, Wien.

Svensson, M.E., Haas, A., 2005. Evolutionary innovation in the vertebrate jaw: a derived morphology in anuran tadpoles and its possible developmental origin. Bioessays 27, 526–532. https://doi.org/10.1002/bies.20224.

Thaler, R., Folly, H., Fadel, R., Alves-Da-Silva, L., Mângia, S., Santana, D.J., 2020. New records of *Lithodytes lineatus* (Anura: Leptodactylidae) in the Cerrado-Amazon transition. Caldasia 42, 157–160. https://doi.org/10.15446/caldasia.v42n1.77257.

Thibaudeau, D.G., Altig, R., 1988. Sequence of ontogenetic development and atrophy of the oral apparatus of six anuran tadpoles. J. Morphol. 197, 63–69. https://doi.org/10.1002/jmor.1051970106.

Valero, K.C.W., Garcia-Porta, J., Rodríguez, A., Arias, M., Shah, A., Randrianiaina, R.D., Brown, J.L., Glaw, F., Amat, F., Künzel, S., Metzler, D., Isokpehi, R.D., Vences, M.D., 2017. Transcriptomic and macroevolutionary evidence for phenotypic uncoupling between frog life history phases. Nat. Commun. 8, 1–9. https://doi.org/10.1038/ncomms15213.

Van Buskirk, J., 2002. A comparative test of the adaptive plasticity hypothesis: relationships between habitat and phenotype in anuran larvae. Am. Nat. 160, 87–102. https://doi.org/10.1086/340599.

Vera Candioti, M.F., 2007. Anatomy of anuran tadpoles from lentic water bodies: systematic relevance and correlation with feeding habits. Zootaxa 1600, 1–175.

Vieira, W.L.S., Santana, G.G., Vieira, K.S., 2007. Description of the tadpole of *Leptodactylus vastus* (Anura, Leptodactylidae). Zootaxa 1529, 61–68. https://doi.org/10.11646/zootaxa.1529.1.5.

Wagler, J., 1830. Natürliches System der Amphibien, mit vorangehender Classification der Säugthiere und Vogel. Ein Beitrag zur vergleichenden Zoologie. München, Stuttgart and Tübingen.

Wassersug, R., Heyer, W.R., 1988. A survey of internal oral features of leptodactylid larvae. Smithsonian Contrib. Zool. 457, 1–99. https://doi.org/10.5479/si.00810282.457.

Wassersug, R.J., 1976. A procedure for differential staining of cartilage and bone in hole formalin fixed vertebrates. Stain Technol. 51, 131–134. https://doi.org/10.3109/10520297609116684.

Wassersug, R.J., 1980. Internal oral features of larvae from eight anuran families: functional, systematic, evolutionary and ecological considerations. Univ. Kans. Misc. Publ. 68, 1–146. https://doi.org/10.5962/bhl.title.16230.

Zaracho, V.H., Kokubum, M.N.C., 2017. Reproduction and larval morphology of *Adenomera diptyx* (Anura: Leptodactylidae) from the Argentinean humid Chaco and Brazilian Pantanal. Salamandra 53, 1–9.